GEOGRAPHICAL REPORTS
OF TOKYO METROPOLITAN UNIVERSITY 55 (2020) 23–34

SEASONAL DIFFERENCES IN THE LAND-ATMOSPHERE COUPLING OVER SOUTH ASIA SIMULATED USING A REGIONAL CLIMATE MODEL

Rakesh Teja KONDURU and Hiroshi G. TAKAHASHI

Abstract This study investigates land-atmosphere coupling over South Asia during the pre-monsoon and monsoon seasons. We conducted three ensemble simulations using the Weather Research and Forecasting (WRF) model (version 3.8.1) as a regional climate model (RCM) coupled with the Noah land surface model (LSM). The default WRF configuration overestimates the roughness length for heat over short vegetation and underestimates the same metric over tall vegetation, leading to a larger sensible heat flux over all South Asia in both aforementioned seasons. This overestimated (underestimated) the strength of the land-atmosphere coupling over larger (smaller) sensible heat flux regions. Dynamically updating the roughness length for heat as a function of canopy height in the LSM results in an error reduction for this variable for different vegetation types. This leads to weaker land-atmosphere coupling for certain regions, resulting in a lower sensible heat flux, in both the pre-monsoon and monsoon seasons. This reduction of sensible heating affects the formation of convection over those regions.

Keywords: land-atmosphere coupling, land surface model, monsoon, pre-monsoon, regional climate model.

1. Introduction

The Asian summer monsoon is influenced by the land-surface characteristics of South Asia. Surface heterogeneity, varying vegetation, and complex topography largely affect the coupling between the land surface and the atmosphere through the exchanges of momentum, moisture, and heat. Accurately simulating land surface and atmosphere coupling in regional and global climate models (GCMs) is essential for resolving regional processes (Takahashi *et al.* 2019).

Previous studies have investigated land-atmosphere coupling by modeling the relationship between soil moisture, evaporation, and precipitation (Zheng *et al.* 2012). For example, Koster *et al.* (2004) found strong coupling hotspots using land-atmosphere coupled climate models. Some studies claim that current climate models unrealistically represent land-atmosphere coupling (Zheng *et al.* 2012). However, the fundamental nature of this coupling i.e., the exchange of energy and water vapor between the land and the atmosphere has not been properly simulated in models. Several studies involving coupled and standalone land surface models (LSMs) report unrealistic simulations of surface energy fluxes.

There are very few studies that address the poor representation of land-atmosphere coupling over the South Asian monsoon region. According to Chakraborty *et al.* (2019), the Noah LSM stand-alone overestimates energy fluxes over the Indo-Gangetic plain of India during the monsoon onset period, contributing to a large dry bias in almost all regional climate modelling (RCMs) and GCMs using this LSM. This misrepresentation of energy fluxes strongly affects the variability of monsoon onset and development. However, a few studies have investigated the simulation of energy fluxes in the coupled Noah LSM over the South Asian monsoon region. Therefore, it is a challenge to thoroughly understand the biases in surface energy fluxes over the South Asian monsoon region in the coupled Noah LSM.

In addition, improving estimations of energy fluxes during the monsoon pre-onset period (Chakraborty *et al.* 2019) in a coupled simulation is necessary. One way of doing this is to tune the parameters in the Noah LSM that govern the computation of fluxes (Zheng *et al.* 2012). However, the heterogeneity of the surface conditions in the South Asian monsoon region should first be considered before tuning the Noah LSM. In the Noah LSM, heterogeneous surfaces are represented by some physical properties, such as surface albedo, roughness length, vegetation fraction, canopy resistance, leaf area index, and canopy height, amongst others. Of these surface physical properties, roughness length plays a major role in the partitioning of surface fluxes. The sensible heat flux is sensitive to the roughness length for heat (Chen and Zhang 2009); however, this has not been investigated specifically over the South Asian monsoon region. This became our motivation to investigate how the roughness length for heat affects surface fluxes over this region.

This study has three goals: (1) to identify discrepancies in surface fluxes in the coupled Noah LSM over the South Asian region for two different seasons, pre-monsoon (April–May) and monsoon (June–September); (2) to discuss the effect of the roughness length for heat on the computation of sensible heat flux; and (3) to compare the modified surface fluxes with those from the default configuration. We did not perform evaluation and verification of surface fluxes against observations because of scarce data over the region. However, we discuss how the behavior of different surface variables is affected due to modifications in the roughness length for heat. In section 2, we give a detailed description of the model setup and datasets used. In section 3, we present results related to model simulations, and in section 4, we discuss the possible impact of modifications in roughness length for heat on convection.

2. Model setup and data

To investigate land-atmosphere coupling, we ran season-long simulations using a non-hydrostatic regional atmospheric model, the Weather Research and Forecasting (WRF) model, version 3.8.1 (Skamarock *et al.* 2008). Our simulations had a spatial resolution of 25 km, with 30 terrain-following vertical levels, for a single domain covering the entire sub-continent of South Asia (65.6–100°E and 5–38°N; Fig. 1a).

Initial and boundary conditions were provided by ERA-interim data (Dee *et al.* 2011), with lateral boundary conditions updated every 6 hours. Daily optimum interpolation sea-surface temperature (Reynolds *et al.* 2007) was also prescribed every 6 hours during the simulations. We chose three contrasting monsoon years: 2007, 2009, and 2012, which were above-normal, drought, and normal years, respectively, based on an India Meteorological Department (IMD) monsoon report (https://www.imd.gov.in/pages/monsoon_main.php).

We used contrasting monsoon years as three ensembles to create an ensemble mean, with the goal of obtaining robust results that are independent of a specific monsoon condition. Including two experiments with 3 ensembles each a total of six simulations were performed from 1 April to 31 October. The first 5 days were excluded from our analysis as model-spin up.

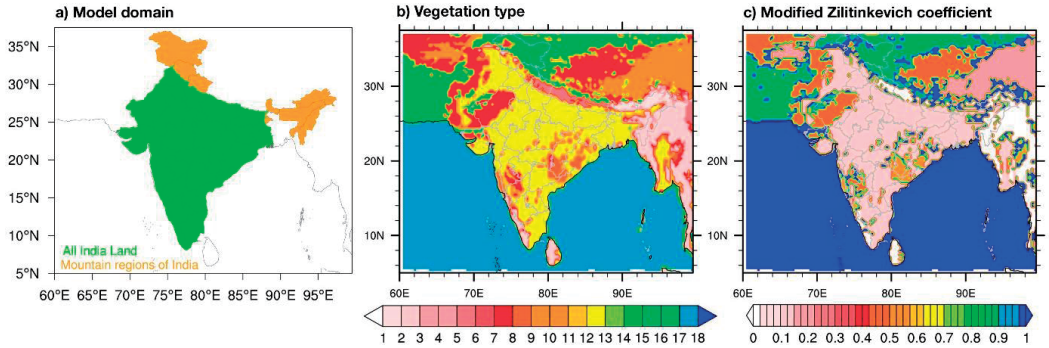

Fig. 1 (a) Simulated model domain, (b) vegetation type used in simulations, and (c) modified Zilitinkevich coefficient (C_{zil}) for the MODIFIED simulations. In (a), the green and orange colored areas represent all Indian land and mountain regions, respectively. Vegetation types in (b) include: 1. evergreen needleleaf forest, 2. evergreen broadleaf forest, 3. deciduous needleleaf forest, 4. deciduous broadleaf forest, 5. mixed forests, 6. closed shrublands, 7. open shrublands, 8. woody savannas, 9. grasslands, 10. permanent wetlands, 11. croplands, 12. urban and built-up areas, 13. cropland/natural vegetation mosaic, 14. snow and ice, 15. barren and sparsely vegetated areas, 16. wood tundra, 17. water and 18. mixed tundra.

For all simulations, we used the Kain-Fritsch cumulus parameterization scheme (Kain 2004), a GCM version of the Rapid Radiative Transfer Model for longwave radiation, and updated Goddard shortwave schemes (Iacono *et al.* 2008). For microphysics, we used the WRF single-moment six-class scheme (Hong *et al.* 2004), and for simulating the planetary boundary layer, we used the Mellor-Yamada-Janić scheme (Mellor and Yamada 1982). The unified Noah land surface physical scheme (Chen and Dudhia 2001) was employed to couple the land surface with the atmosphere. With these settings as our default configuration, we performed control simulations (CTRL). In another set of simulations, we modified the surface flux computation in the Noah LSM (MODIFIED).

The model-simulated surface temperature was evaluated using the IMD gridded surface temperature dataset, available at a 50-km resolution over the Indian region (Srivastava *et al.* 2009). We obtained these surface temperature data for our study period: 2007, 2009, and 2012, during the pre-monsoon (April–May) and monsoon (June–September) seasons.

Modification of surface flux computation

In the Noah LSM, surface fluxes are computed with a bulk aerodynamic method, by integrating from the reference surface up to the roughness length. Sensible heat flux (*SH*, in W m^{-2}) was calculated based on the surface potential temperature (θ_s) and air potential temperature (θ_a) in the surface layer, as follows:

$$SH = \rho c_p C_h U(\theta_s - \theta_a), \quad (1)$$

Where,

$$C_h = \frac{k^2/R}{\left[\ln\left(\frac{Z}{Z_{0m}}\right) - \psi_m\left(\frac{Z}{L}\right) + \psi_m\left(\frac{Z_{0m}}{L}\right)\right]\left[\ln\left(\frac{Z}{Z_{0t}}\right) - \psi_t\left(\frac{Z}{L}\right) + \psi_t\left(\frac{Z_{0t}}{L}\right)\right]}, \quad (2)$$

and ρ is air density; c_p is specific heat capacity; U is mean wind speed; k = 0.4 is the von Kármán constant; R = 1.0 is the turbulent Prandtl number; z is measurement height; ψ_m and ψ_t are the stability correction functions for momentum and sensible heat transfer, respectively; L is the Monin-Obukhov length; ; and the subscripts 0, m, and t refer to the reference surface, momentum, and heat, respectively. C_h is known as the surface exchange coefficient for heat transfer and controls coupling between the land surface and the atmosphere (Chen and Zhang 2009). According to LeMone *et al.* (2008), modifying the surface exchange coefficient for heat largely affects estimations of sensible heat flux. Therefore, we modified the surface exchange coefficient for heat and analyzed coupling strength over the Indian monsoon region in two different climate regimes: pre-monsoon and monsoon.

Note that C_h mainly depends upon the roughness lengths for momentum (Z_{0m}) and heat (Z_{0t}). Zilitinkevich (1972) proposed a relationship between these two as a function of atmospheric turbulence, which is used in the Noah LSM, as follows:

$$Z_{0t} = Z_{0m} e^{\left(-kC_{zil}\sqrt{R_e}\right)}, \quad (3)$$

where R_e is the roughness Reynolds number, and C_{zil} is an unknown parameter specified as 0.1 in the Noah LSM. From Eq. (3), it is clear that C_{zil} is an important parameter for determining Z_{0t}. According to Chen and Zhang (2009), the default value of C_{zil} results in the Noah LSM being unable to simulate seasonal variations in Z_{0t}. As a result, they introduced seasonal variations in C_{zil} based on Z_{0m}, in the standalone Noah LSM as follows:

$$C_{zil} = 10^{-0.4\frac{Z_{0m}}{0.07}}, \quad (4)$$

They found that seasonal variations in vegetation (Fig. 1b) indirectly affected Z_{0t} and thus, C_h. Canopy height in the model was computed indirectly based on the roughness length for momentum. It should be noted that such a modification of C_{zil} was not implemented in the recent standalone Noah LSM version 3.7.1, nor the coupled Noah LSM (Chen and Zhang 2009). Therefore, we were the first to implement these modifications in roughness length for heat by varying C_{zil} (Fig. 1c) in the coupled Noah LSM (MODIFIED), and to allow this to affect calculations of C_h.

3. Results

Evaluation of surface temperatures between CTRL and observations

We evaluated the downscaled WRF simulations using the seasonal (pre-monsoon and monsoon) mean surface temperature for three years, comparing the ensemble mean with the IMD observations. The ensemble mean temperature of the observations was higher (> 33°C) during the pre-monsoon season and lower (< 30°C) during the monsoon season (Fig. 2). This difference clearly explained the dry pre-monsoon and wet monsoon season. The model simulations have substantially simulated the seasonal temperatures aside from some over- and under-estimations. Modeled surface temperatures were too high over central India for both seasons, but the errors were larger (1–3°C) during the monsoon. During the pre-monsoon season, surface temperatures were underestimated (by 1–2°C) along the western and southeastern coast of India. For western India climatologically a very hot region, temperatures were underestimated by 2–3°C. Over mountain regions such as the Western Ghats and northeastern India, surface temperatures were also underestimated by the model.

Differences between MODIFIED and CTRL simulations

We compared simulated surface temperatures from the MODIFIED and CTRL experiments for the pre-monsoon and monsoon seasons (Figs. 3a and 3b). The MODIFIED experiment simulated higher surface temperatures than the CTRL experiment over the Indian region for both seasons. A larger difference (~ 3–5°C) in surface temperatures was noticeable

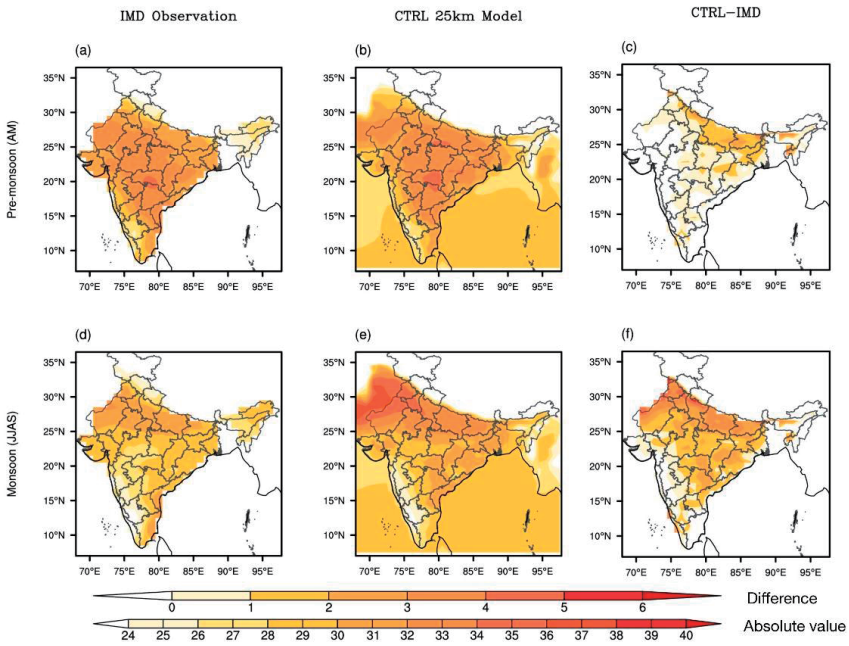

Fig. 2 Ensemble mean surface temperature (°C) from the India Meteorological Department (IMD) gridded observations (a, d) and model simulations (b, e) for the pre-monsoon and monsoon seasons. The differences between observations and model simulations are also shown (c, f). The unit of the model simulated surface temperatures is °C.

during the pre-monsoon season for central India. Consequently, the MODIFIED simulations reduced the underestimation of surface temperatures that was seen in the CTRL runs. However, there was a small underestimation of surface temperatures for the Western Ghats and northeast mountainous regions for both seasons. This underestimation of surface temperature in the model affected the surface fluxes.

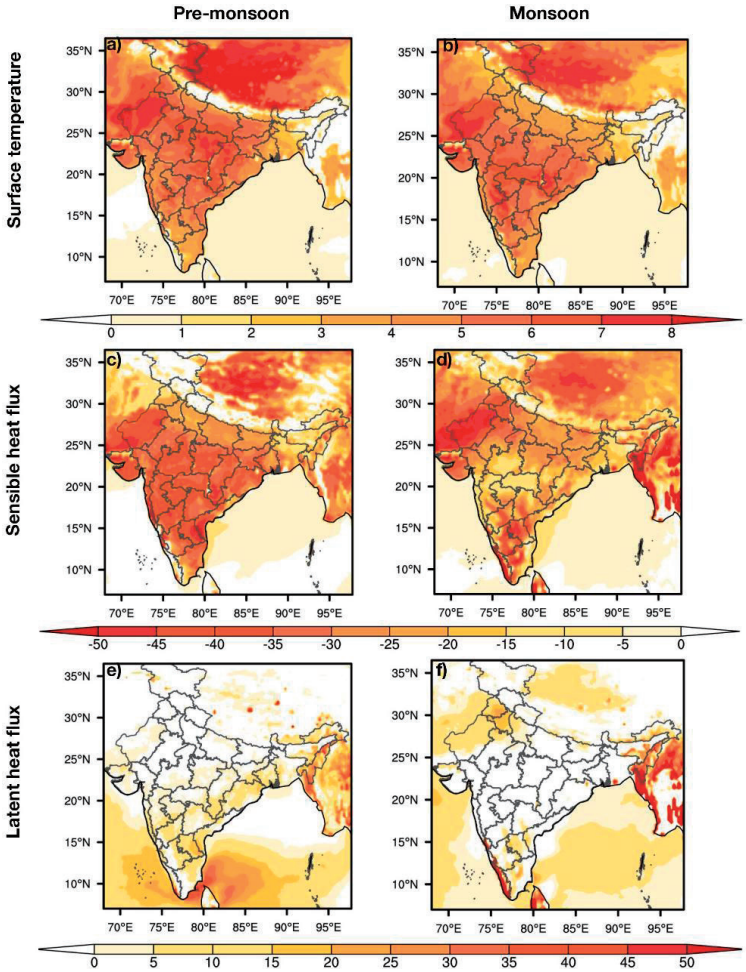

Fig. 3 Differences between the MODIFIED and CTRL simulations during the pre-monsoon and monsoon seasons: (a, b) ensemble mean surface temperature (°C), (c, d) sensible heat flux (W m^{-2}), and (e, f) latent heat flux (W m^{-2}). The ensemble mean was computed based on all three years: 2007, 2009, and 2012.

To diagnose changes in the surface heat fluxes in the MODIFIED simulations, we analyzed the difference between the MODIFIED and CTRL seasonal means of sensible heat flux (Figs. 3c and 3d) and latent heat flux (Figs. 3e and 3f). The sensible heat flux in the CTRL simulations was higher than that in the MODIFIED experiment for both seasons. In the MODIFED experiment, the sensible heat flux exhibited a clear reduction of 20–40 W m^{-2}

over all of India. However, there was an increase in sensible heat flux for the western Ghats and northeast mountainous regions. The latent heat flux exhibited different trends for the two seasons. During the pre-monsoon season, the latent heat flux increased by 5–20 W m^{-2} over all of India, apart from in the northwest, and the Western Ghats. However, during the monsoon, the latent heat flux increased over western India, along the mountains of northeastern India, and for the Western Ghats. Simultaneously, it decreased over the central and southeast coast of India.

Impact of land-atmosphere coupling on surface fluxes

In the model, land-atmosphere coupling is essentially represented by C_h in the sensible heat flux calculation. We calculated C_h as described in Eqs. (1) and (2) for both the pre-monsoon and monsoon seasons (Fig. 4). The CTRL experiment simulates a higher C_h over India for both seasons, leading to higher sensible heat flux. This is consistent with the results of Chen and Zhang (2009). A higher C_h suggests that the land and the atmosphere are more

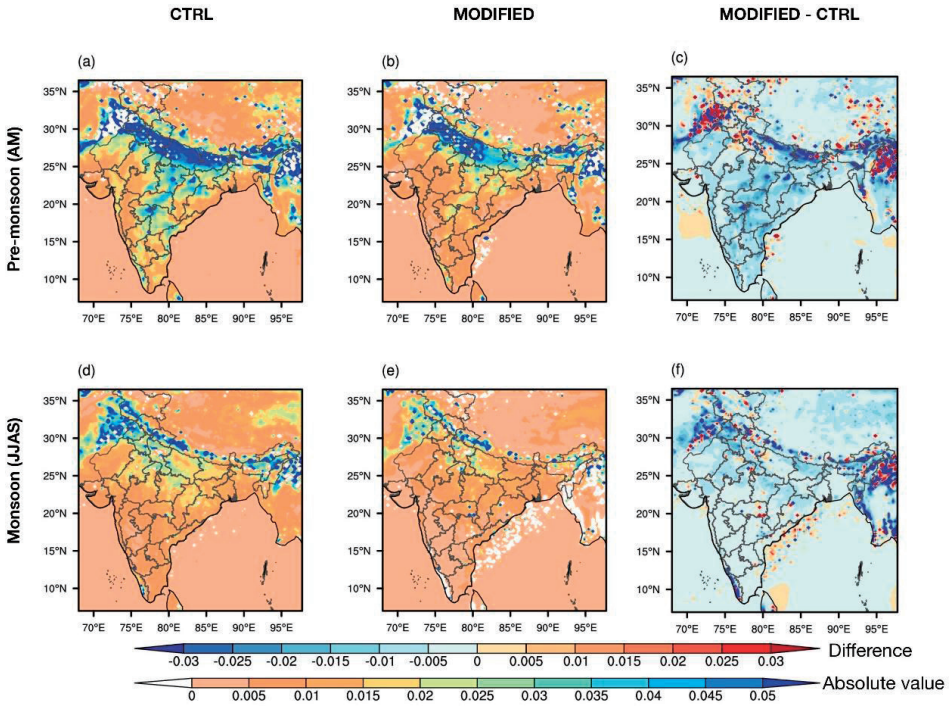

Fig. 4 Surface exchange coefficient (C_h) ensemble mean for the CTRL (first column) and MODIFIED (second column) experiments during the pre-monsoon and monsoon seasons. The difference between the MODIFIED and CTRL output is shown in the third column. The ensemble mean was computed for all three years: 2007, 2009, 2012.

strongly coupled. When coupling strength was compared for each of the two seasons, coupling was stronger during the pre-monsoon season than during the monsoon over central India, along the foothills of the Himalayas, and over the mountains of the Western Ghats and northeast India. A higher C_h is associated with a higher roughness length for heat irrespective

of canopy type (Figs. 5a and 5b), and this increases sensible heat flux. Note that short vegetation such as croplands or grasslands, which covers 80% of the Indian region (Fig. 1b), is usually associated with a lower roughness length for heat. Because C_{zil} (= 0.1) was kept constant in the CTRL simulations, the roughness length for heat was overestimated for short vegetation and underestimated for regions with tall vegetation such as the forests of the Western Ghats and northeast India.

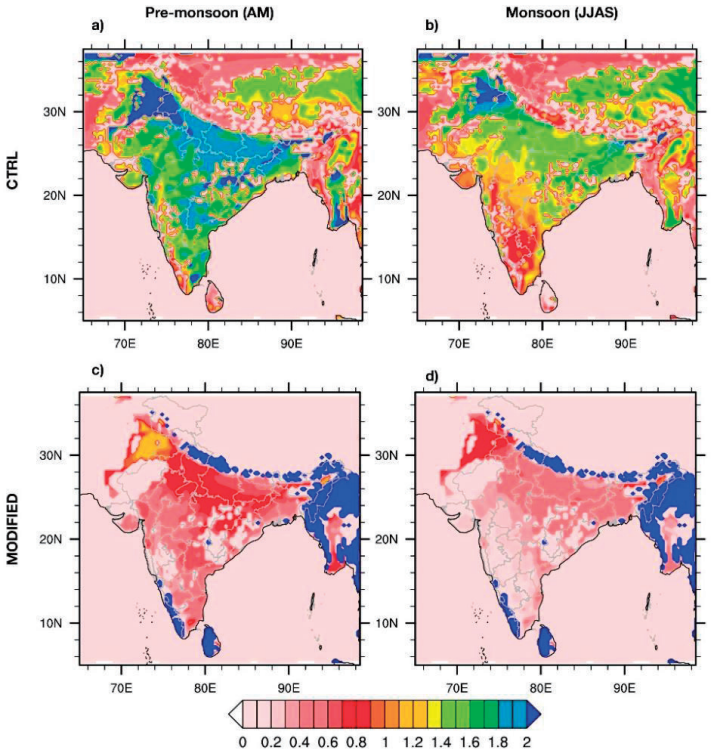

Fig. 5 Roughness length for heat (m) for the CTRL (a, b) and MODIFIED (c, d) simulations during the pre-monsoon (a, c) and monsoon (b, d) seasons.

The roughness length for heat was reduced (Figs. 5c and 5d) when C_{zil} was updated dynamically as a function of canopy height, as in the MODIFIED simulations, thereby affecting C_h values. Over the Indian region, C_h values were lower in the MODIFIED simulations than in the CTRL simulations for both seasons, which therefore resulted in decreased land-atmosphere coupling. A large decrease in C_h was noticeable over central India, and along the mountains of northeast India and the Himalayan foothills. A decrease in the roughness length for heat was related to higher C_{zil} (Fig. 1c). In the MODIFIED simulations, values of C_{zil} were greater than 0.1 (its value in the CTRL). According to LeMone *et al.* (2008; see Fig 18 in this paper), when C_{zil} <0.1, C_h increases exponentially, hence strong land-atmosphere coupling occurs. When C_{zil} >0.1, C_h decreases, and thus coupling strength decreases. C_{zil} and C_h values in the MODIFIED simulations were consistent with those used by LeMone *et al.* (2008). In particular, the MODIFIED

simulations showed that there was a clear difference in C_{zil} and C_h with canopy height (Figs. 1b, 1c and 4). For the MODIFIED experiment, short vegetation (croplands or grasslands) was associated with higher C_{zil} and lower C_h values than in the CTRL experiment, pointing to weaker land-atmosphere coupling. For tall vegetation in mountainous regions such as the Western Ghats and northeast India, C_{zil} and C_h values were lower and higher, respectively, suggesting strong coupling.

4. Response of convection to coupling strength modification

From section 3 in both seasons, the MODIFIED experiment simulated reduced land-atmosphere coupling, C_h, and sensible heat flux. Also, a large increase in the latent heat flux was found for southeastern India, along the Western Ghats mountains, and in northeast India,

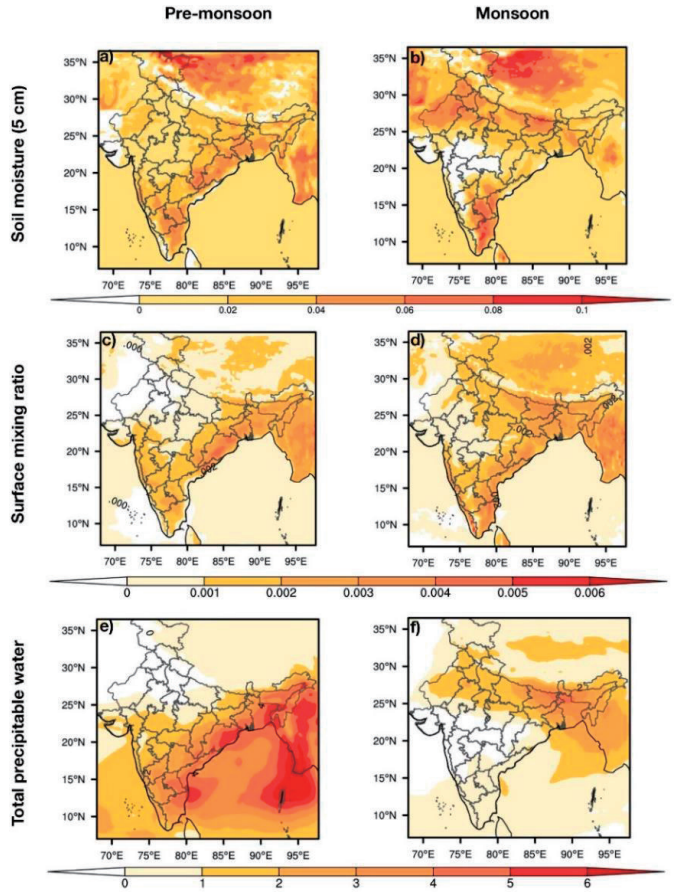

Fig. 6 Differences between the MODIFIED and CTRL simulations during the pre-monsoon and monsoon seasons: (a, b) ensemble mean soil moisture (m^3 m^{-3}), (c, d) surface mixing ratio (kg kg^{-1}), and (e, f) total precipitable water vapor (mm). The ensemble mean was computed based on all three years: 2007, 2009, and 2012.

in both seasons. In addition, the downward ground heat flux increased (not shown) in correspondence with an increase in surface skin temperature, due to an imbalance with net radiation and ground heat flux. We investigated the impact of these heat flux changes on convection during the two seasons.

To illustrate the response of convection, we presented the differences between the MODIFIED and CTRL ensemble means of soil moisture (at a 5-cm depth below the surface; $m^3\ m^{-3}$), surface mixing ratio, and total precipitable water (Fig. 6). During the pre-monsoon season, positive anomalies of the surface mixing ratio, soil moisture, and total precipitable water were simulated in the MODIFIED experiment along the eastern coast of India, southern India, the Western Ghats, and northeast India. The increased availability of moisture along with a higher latent heat flux supported an increase in convection for these regions, in agreement with the results of Takahashi *et al.* (2019). Similarly, during the monsoon season, the MODIFIED experiment indicated that surface moisture increased over central India, western India, the southeastern coast, and northeast India. As a result, the moist environment together with a lower sensible heat flux favored convection during the monsoon. Consequently, precipitation for those regions might increase in the MODIFIED simulations.

5. Summary and conclusions

To understand land-atmosphere coupling over South Asia, we investigated the reproducibility of surface heat fluxes during the pre-monsoon and monsoon seasons, using an RCM. We have conducted six simulations with three ensembles each for two experiments using the WRF model coupled to the Noah LSM. In the CTRL simulations (default configuration of the WRF model), we found that land-atmosphere coupling was overestimated over all the South Asian region due to an overestimation of roughness length for heat for different vegetation types. Because the roughness length for heat was higher, the sensible heat flux was overestimated in both seasons over all South Asia.

To address this issue, we dynamically updated C_{zil} as a function of canopy height in the Noah LSM. Canopy height is modeled indirectly based on the roughness length for momentum. This modification results in a decrease in the roughness length for heat over short vegetation types and an increase in the same metric over tall vegetation. In the MODIFIED simulations, land-atmosphere coupling was weaker for regions where the roughness length for heat was small; thus, a smaller sensible heat flux was predicted for both the pre-monsoon and monsoon seasons. As a result, the availability of surface moisture increased for both seasons, contributing to an increase in convective activity over South Asia. The experiments in this investigation showed that there was a clear difference in surface fluxes between the CTRL and MODIFIED simulations. In the future, these results can be verified and evaluated using season-long surface observations.

Acknowledgements

This work was partly supported by JSPS KAKENHI Grant Number 19H01375, Japan Aerospace Exploration Agency (JAXA) EO-RA2 (PI number: ER2GPF012), and by the “Tokyo Human Resources Fund for City Diplomacy” from the Tokyo Metropolitan

Government, Japan. We thank the India Meteorological Department (IMD) for providing the gridded precipitation data sets. The Era-Interim data are obtained via the European Center for Medium-range Weather Forecasts public reanalysis-data sets web interface (https://www.ecmwf.int/en/forecasts/datasets). The OISST v2 data are obtained from the online website of the NOAA Earth System Research Laboratory's Physical Sciences Division (https://www.ncdc.noaa.gov/oisst).

References

Chakraborty, T., Sarangi, C., Krishnan, M., Tripathi, S. N., Morrison, R., and Evans, J. 2019. Biases in the model simulated surface-energy fluxes during the Indian monsoon onset period. *Boundary Layer Meteorology* **170**: 323–341.

Chen, F., and Zhang, Y. 2009. On the coupling strength between the land surface and the atmosphere: from viewpoint of surface exchange coefficient. *Geophysical Research Letters* **36**: L10404.

Chen, F., and Dudhia, J. 2001. Coupling an advanced land surface–hydrology model with the Penn State–NCAR MM5 modeling system. Part I: Model implementation and sensitivity. *Monthly Weather Reviews* **129**: 569−585.

Dee, D. P., Uppala, S. M., Simmons, A. J., Berrisford, P., Poli, P., Kobayashi, S., Andrae, U., Balmaseda, M. A., Balsamo, G., Bauer, P., Bechtold, P., Beljaars, A. C. M., Berg, L. V. D., Bidlot, J., Bormann, N., Delsol, C., Dragani, R., Fuentes, M., Geer, A. J., Haimberger, L., Healy, S. B.Herbach, H., Hólm, E. V., Isaksen, L., Kallberg, P., Köhler, M., Matricardi, M., McNally, A. P., Mong-Sanz, B. M., Morcrette, J. -J., Park, B. -K., Peubey, C., de Rosnay, P., Tavolato, C., Thépaut, J. -N., and Vitart, F. 2011. The ERA-Interim reanalysis: Configuration and performance of the data assimilation system. *Quarterly Journal of the Royal Meteorological Society* **137**: 553−597.

Hong, S. Y., Dudhia, J., and Chen, S. H. 2004. A revised approach to ice microphysical processes for the bulk parameterization of clouds and precipitation. *Monthly Weather Review* **132**: 103−120.

Iacono, M. J., Delamere, J. S., Mlawer, E. J., Shephard, M. W., Clough, S. A., and Collins, W. D. 2008. Radiative forcing by long-lived greenhouse gases: Calculations with the AER radiative transfer models. *Journal of Geophysical Research* **113**: D13103.

Kain, J. S. 2004. The Kain–Fritsch convective parameterization: an update. *Journal of Applied Meteorology*. **43**: 170−181.

Koster, R. D., Dirmeyer, P. A., Guo, Z., Bonan, G., Chan, E., Cox, P., Gordon, C. T., Kanae, S., Kowalczyk, E., Lawrence, D., Liu, P., Lu, C. H., Malyshev, S., McAvaney, B., Mitchell, K., Mocko, D., Oki, T., Oleson, K., Pitman, A., Sud, Y. C., Taylor, C. M., Verseghy, D., Vasic, R., Xue, Y., and Yamada, T. 2004. Regions of strong coupling between soil moisture and precipitation, *Science* **305**: 1138−1141.

LeMone, M. A., Tewari, M., Chen, F., Alfieri, J. G., and Niyogi, D. 2008. Evaluation of the Noah land surface model using data from a fair-weather IHOP_2002 day with heterogeneous surface fluxes. *Monthly Weather Review* **136**: 4915–4951.

Mellor, G. L., and Yamada, T. 1982. Development of a turbulence closure model for geophysical fluid problems. *Review of Geophysics* **20**: 851–875.

Reynolds, R.W., Smith, T.M., Liu, C., Chelton, D.B., Casey, K.S. and Schlax, M.G. 2007. Daily high-resolution-blended analyses for sea surface temperature. *Journal of Climate*, **20**: 5473–5496.

Skamarock, W. C., Klemp, J. B., Dudhia, J., Gill, D. O., Barker, D. M., Duda, M. G., Huang, X. Y., Wang, W., and Powers, J. G. 2008. A description of the Advanced Research WRF version 3, NCAR Tech. Note NCAR/TN-475+STR, 113 pp.

Srivastava, A. K., Rajeevan, M., and Kshirsagar, S. R. 2009. Development of a high resolution daily gridded temperature dataset (1969-2005) for the Indian region. *Atmospheric Science Letters* **10**: 249–254.

Takahashi, H. G., and Polcher, J. 2019. Weakening of rainfall intensity on wet soils over the wet Asian monsoon region using a high-resolution regional climate model. *Progress in Earth and Planetary Science* **6**: 26.

Zheng, W., Wei, H., Wang, Z., Zeng, X., Meng, J., Ek, M., Mitchell, K., and Derber, J. 2012. Improvement of daytime land surface skin temperature over arid regions in the NCEP GFS model and its impact on the satellite data assimilation. *Journal of Geographical Research: Atmosphere* **117**: D06117.

Zilitinkevich, S. S. 1972. On the determination of the height of the Ekman boundary layer. *Boundary Layer Meteorology* **3**: 141–145.